

Electrowetting on functional fibers - Supplementary Informations

R. Dufour,^{a,b} A. Dibao-Dina,^{a,b} M. Harnois,^{a,b} X. Tao,^{a,c} C. Dufour,^{a,b} R. Boukherroub,^{a,d} V. Senez^{a,b}
and V. Thomy*^{a,b}

1 Movies

- Movie M1 shows EWOD actuation of a 1 μL water droplet for $V_{rms} = 48$ and 96 V.
- Movie M2 shows EWOD actuation of a 1 μL water droplet for $V_{rms} = 160$ V. At this high voltage, hydrodynamic instabilities are observed (emission of satellite droplets).
- Movie M3 show the operation of an EWOD controlled fluidic diode, consisting in a junction between two fibers. Actuation sequence is off-on-off-off-on-on.

2 Contact angle and drop volume measurement

2.1 Contact angles measurement

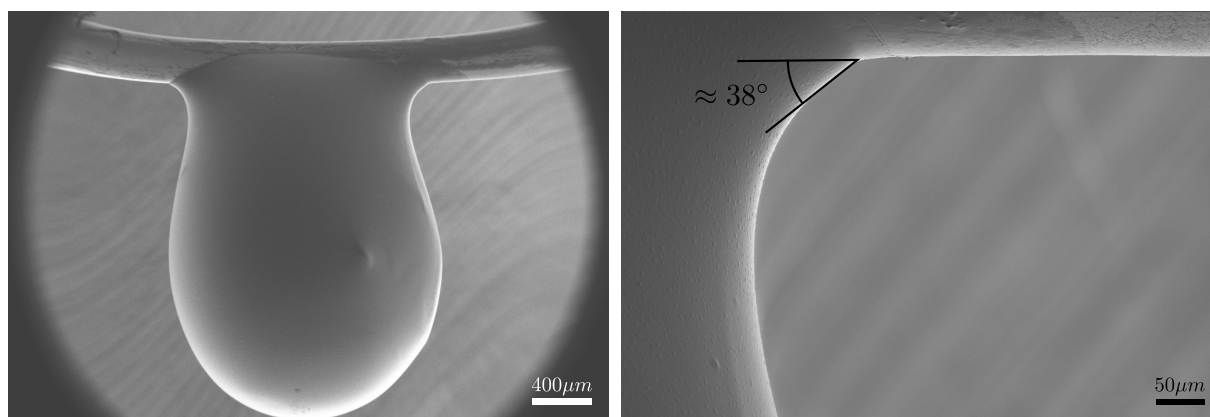


Fig. 1 SEM observation of a hanging NOA droplet. Right image depicts the continuous variation of liquid-air interface from a microscopic equilibrium angle to the macroscopic shape.

Measurement of contact angles of clam-shell drops hanging on horizontal fibers is not straightforward compared to classical studies on smooth or textured surfaces.^{1,2} Because of the complex drop shape, the interface profile continuously varies from a microscopic contact angle to the macroscopic drop profile.

^a University Lille Nord de France, Villeneuve d'Ascq, France

^b Institute of Electronics, Microelectronics and Nanotechnology (IEMN), UMR CNRS 8520, Villeneuve d'Ascq, France; E-mail: vincent.thomy@iemn.univ-lille1.fr

^c Laboratory for Textile Material Engineering (GEMTEX), National Graduate School of Textile Engineering (ENSAIT), 59056 Roubaix, France

^d Interdisciplinary Research Institute (IRI), USR CNRS 3078, Parc de la Haute Borne, Avenue de Halley, 59658 Villeneuve d'Ascq, France

* Corresponding author: vincent.thomy@iemn.univ-lille1.fr

Accurate evaluation of θ is particularly tricky for wetting liquid as depicted in figure 1 for a hanging NOA droplet. Low surface tension of NOA ($\approx 40\text{mN/m}$) results in $\theta \approx 40^\circ$ and a very high magnification is necessary to capture the microscopic angle. The distortion is less significant as far as hydrophobic fibers are concerned. Indeed as shown in figure 2, the local apparent contact angle can be properly measured within a $200\ \mu\text{m}$ windows around the contact line, the standard error over all measurement is $\approx \pm 2^\circ$.

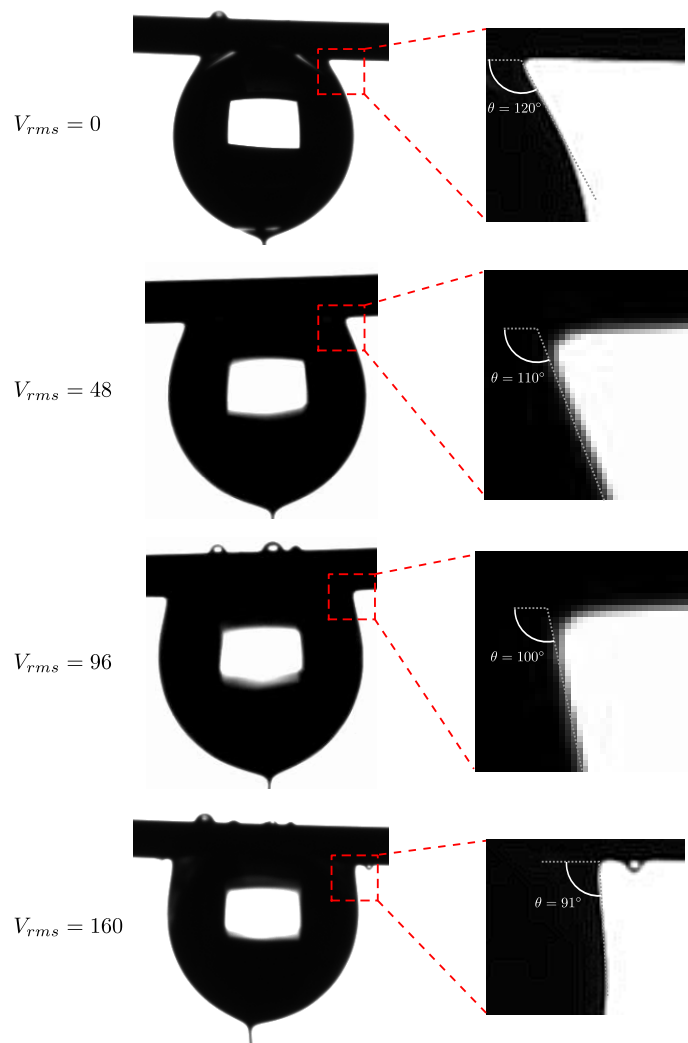


Fig. 2 Measurement of contact angles for water drops on fibers under EWOD actuation for $V_{RMS} = 0, 48, 96$ and 160 V. Magnifications show the measured contact angles.

Another usual error in measured contact angle results from a displacement of the drop along the axis of the camera (i.e. rotation around the fiber). For that reason, it is necessary to use a second camera recording a lateral view of the drop. Computing the gravity center displacement during the experiment enables to make sure that the drop only moves upward.

2.2 Drop volume estimation

Concerning the measurement of maximal drop volumes (Ω_c), there is no direct method to compute the volume from side view of barrel-shaped drops. Consequently, the volumes were average assuming a rotational symmetry and computed with DSA3 drop shape analysis software. The so-called ‘pendant drop’ method was used to capture the drop shape and compute Ω . The accuracy of this approximation was estimated as follow : (i) Drops of volume $\Omega \leq \Omega_c$ were simulated with Surface Evolver for a fiber radius $r = 117\mu\text{m}$ and $80 < \theta < 120$. (ii) Side-views were created from simulation results and loaded in DSA3 software. (iii) Drop volume was computed using rotational symmetry approximation and compared to real drop volume. Results are shown in figure 3 and show that this approximation leads to less than 10 % error.

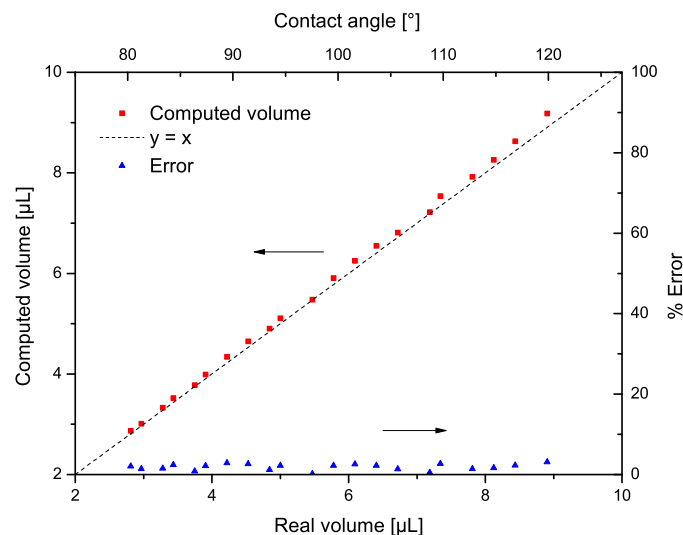


Fig. 3 Estimation of rotational symmetry approximation accuracy for the measurement of drop volumes. The top/bottom x axis corresponds to simulated volumes close to Ω_c associated with contact angles ranging from 0 to 180° . The left y axis corresponds to volumes measured from side views of the simulated droplets. Measurement error is shown on the right y axis

It is to be noted that for drop volumes much lower than Ω_c this approximation no longer holds and measurement error quickly increases above 10%.

3 Variation of drop contact length upon EWOD actuation

Figure 4 shows the variation of drop contact length on the fiber as a function of the applied voltage. Variation of contact length appears to be very similar to variation of contact angle. In a first time the droplet quickly spreads. Then starting from $V^2 \approx 64 \text{ V}$, spreading continues but more slowly and we do not observe a clear saturation as it is the case for planar EWOD. Once voltage is switched off (from 160 to 0 V), contact length recover its initial value, as do the contact angle.

4 Relationship between maximum drop volume Ω_M and applied voltage V

A first step toward analytical calculation of Ω_M was previously performed by E. Lorenceau et al.³. However they considered barrel shaped droplets on wetting fibers ($\theta = 0$) and focused on the variation of Ω_M with respect to the fiber radius. In their analysis they assumed that ‘ the force resulting from the horizontal fiber

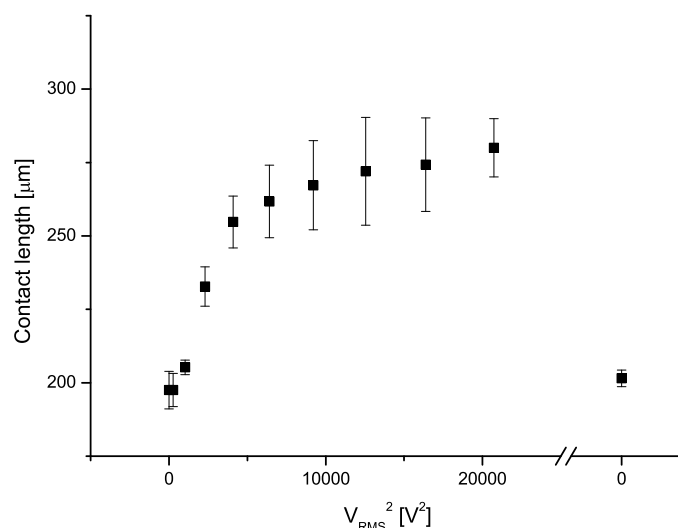


Fig. 4 Variation of drop contact length as a function of applied voltage.

is equivalent to the force generated by two similar fibers [...] pointing radially.', which is represented in figure 5. Following this approach and considering a fiber for which $\theta = 0$, the maximal capillary force exerted by the two fibers as $\alpha \rightarrow \frac{\pi}{2}$ is $F_{C,MAX} = 4\pi b\gamma$. Balancing this force with the drop weight leads to the following expression for Ω_M :

$$\Omega_M \approx \frac{4\pi b\gamma}{\rho g}$$

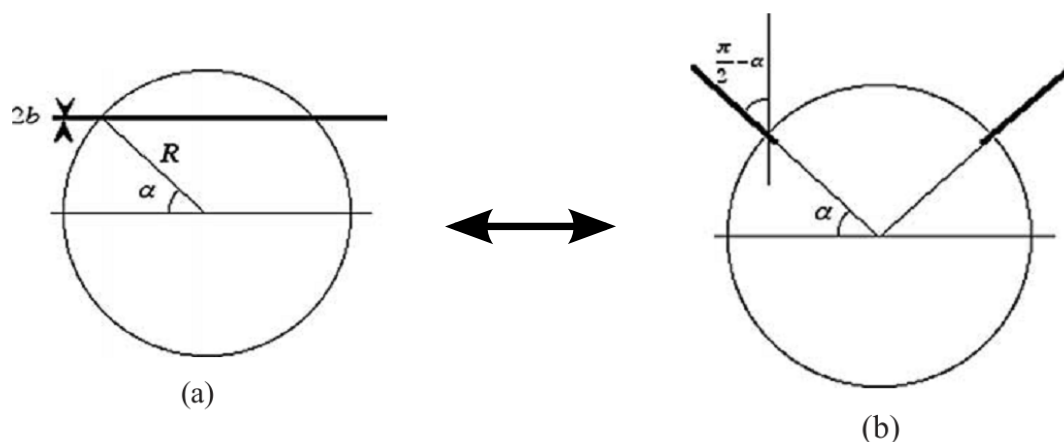


Fig. 5 Point of view of E. Lorenceau et al. concerning the force exerted by a fiber on a barrel shaped droplet. The force exerted by the horizontal fiber is equivalent to the force exerted by two fibers pointing radially³.

As far as our fibers are concerned, it is not rigorous to use such an analytical approach. Indeed in the aforementioned work, the oil droplets exhibit a barrel configuration (liquid wraps around the fiber, so contact line is separated into two roughly circular parts). Such configuration makes possible the assumption of figure 5 (capillary force exerted by the fiber on the drop is focused at two contact points, and thus is analogous to the force generated by two fibers pointing radially).

On the other hand, our water droplets on hydrophobic fibers exhibit a barrel shape with a single continuous contact line. In that case the capillary force exerted by the fiber is distributed all along the perimeter of drop fiber contacting surface and is not likely to be expressed in such a way. It is to be noted that a simple correction factor to the capillary force such as would here leads to a downward force since $\theta > 90^\circ$ on the hydrophobic fiber.

Thereby it is not straightforward to analytically predict the scaling law relating Ω_M and θ . All we can eventually do is to use numerical simulation results to display the $\Omega_M = f(\theta)$ relationship, which is shown on the graph of figure 6. In the range of computed parameters ($80^\circ < \theta < 120^\circ$), a linear behavior is clearly observed between the two quantities, with $R^2 > 0.99$. For the $117 \mu\text{m}$ in diameter fiber, slope is $9.15 \mu\text{L}^{-1}$ and intercept equals $7.11 \mu\text{L}$ (corresponding to $\theta = \frac{\pi}{2}$). Thereby from this point we can assume that the maximal hanging drop volume follows the scaling law $\Omega_M \propto \cos \theta$. It is to be noted that rigorous derivation of this result is still to be done, and that this linear behavior is here demonstrated only for a limited contact angle range.

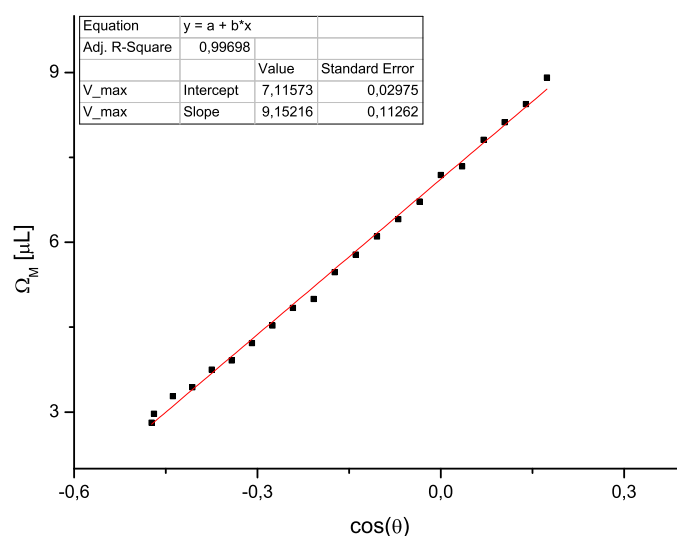


Fig. 6 $\Omega_M = f(\theta)$ relationship obtained from numerical simulations of a water droplet on a $117 \mu\text{m}$ in diameter fiber.

In a second time, using the Young-Duprè relationship, we could expect $\cos \theta \propto V^2$. However, it is clearly observed in the case of EWOD on fiber, that the EWOD response hardly follows the Young-Duprè approximation (it is the case only for small V values, i.e. up to $V_{rms} \approx 64 V$, cf. figure 4 in the manuscript). As a consequence, there is no reason for Ω_M to linearly increase with V^2 over the whole voltage range.

In order to give to the reader an idea about the amplitude of the modulation (in $\mu\text{L}\cdot\text{V}^{-1}$ or $\mu\text{L}\cdot\text{V}^{-2}$), figure 7 represents linear curve fitting for $\Omega_M = f(V_{rms})$ and $\Omega_M = f(V_{rms}^2)$ relationships. The second case exhibits a better correlation with $R^2 = 0.87$ instead of $R^2 = 0.70$ for the former case.

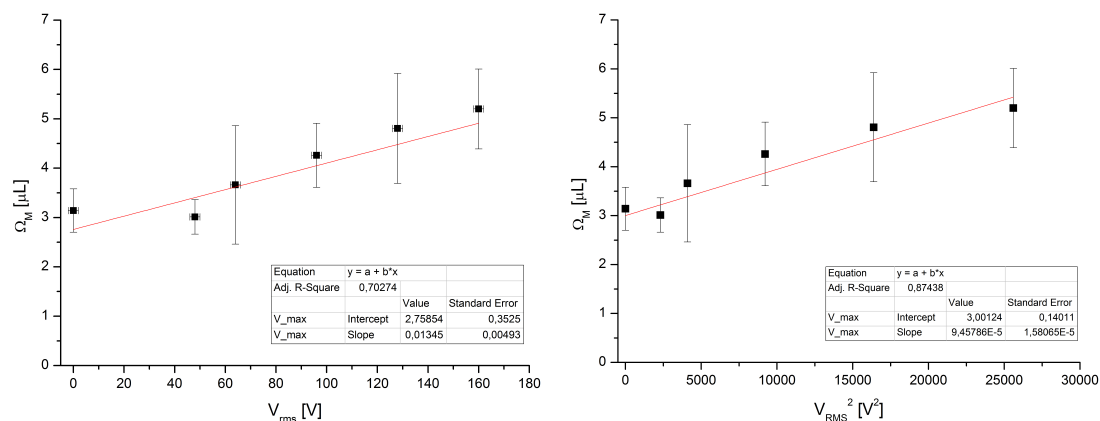


Fig. 7 Linear curve fitting for $\Omega_M = f(V_{rms})$ and $\Omega_M = f(V_{rms}^2)$ relationships.

5 Surface evolver simulations

The Surface Evolver is an interactive program for the study of surfaces shaped by surface tension and other energies. A surface is implemented as a union of triangles and evolved toward minimal energy by a gradient descent method.

In the case of a drop hanging on a fiber, the total energy E results from interfacial and gravitational contributions which are computed using surface and line integrals. Moreover the surface is subjected to volume and boundary constraints.

5.1 Initial geometry and constraints

Taking advantage of symmetries, only a quarter of the drop is modelled. Initial geometry is represented in figure 8 (The fiber aligns with the x axis). It consists of 7 vertices, 16 edges and 6 faces, the following constraints and symmetries are applied :

- Symmetry with respect to yOz plane (edges 4,11)
Equation : $x = 0$
- Symmetry with respect to xOz plane (edge 16)
Equation : $y = 0$
- Confinement to fiber surface (edges 9,14)
Equation : $y^2 + z^2 = R^2$, with R the fiber radius

5.2 Volume and energies computation

Interfacial energies and contact angle The energy E_{LV} corresponding to the liquid - air interface is directly calculated from the surface of facets (This is automatically done by Evolver when assigning an interfacial energy γ_{LV} to the facets).

The solid - liquid interfacial tension γ_{SL} is obtained from γ_{LV} and θ through the Young relationship : $\gamma_{SL} = \gamma_{LV} \cdot \cos \theta$ (the solid - vapor interface is not represented so $\gamma_{SV} = 0$). Since the liquid - fiber contacting

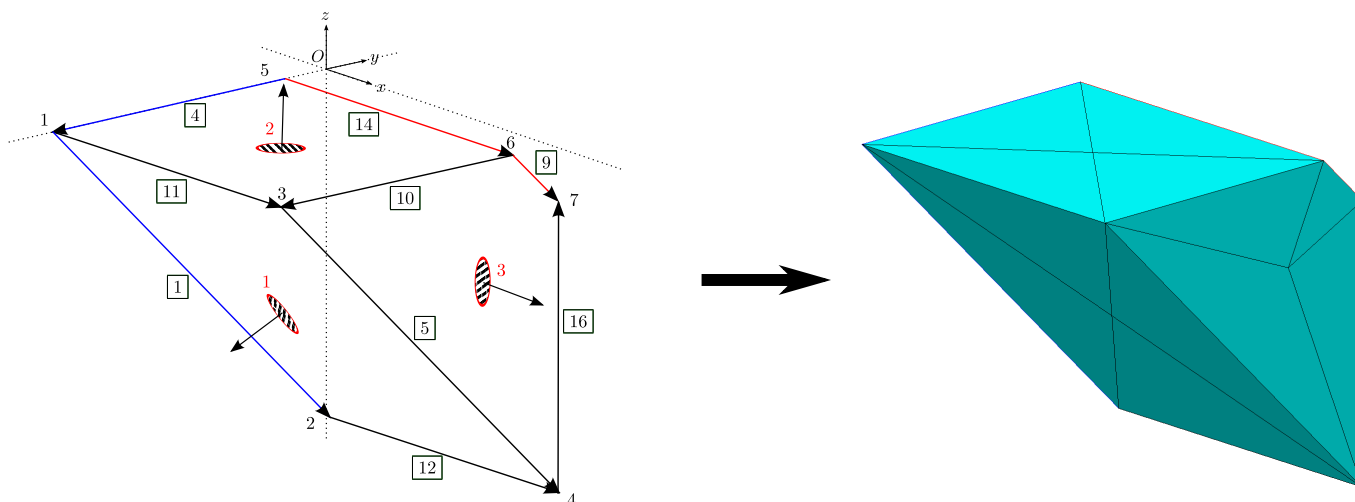


Fig. 8 The initial drop geometry consists of 7 vertices, 16 edges and 6 faces. A first symmetry constraint is applied to edges 1 and 4 (Oyz plane). A second symmetry constraint is applied to edge 16 (Oxz plane). The liquid - fiber contacting surface is not represented and the corresponding energy is taken into account using a line integral along the contact line (edges 9 and 14 in red).

surface is not modelled, the corresponding energy E_{SL} is obtained from a line integral along the contact line. Considering cylindrical coordinates (r, θ, x) , E_{SL} can be written :

$$E_{SL} = \gamma_{SL} \int_C R.x. d\theta \quad (1)$$

Where curve C corresponds to the contact line of the drop on the fiber. Since $R = \sqrt{y^2 + z^2}$, this integral can be re-written :

$$E_{SL} = \gamma_{SL} \int_C \frac{y^2 + z^2}{R}.x. d\theta = \gamma_{SL} \int_C x.\frac{y}{R}.y. d\theta + x.\frac{z}{R}.z. d\theta \quad (2)$$

Finally, from $y = R.\cos\theta$ and $z = R.\sin\theta$, we introduce the following relationships :

$$dy = -z.d\theta \quad (3)$$

$$dz = y.d\theta \quad (4)$$

Which enables to compute E_{SL} in Evolver cartesian coordinate system through the following vector integral:

$$E_{SL} = \gamma_{SL} \int_C x.\frac{y}{R}.dz + x.\frac{z}{R}.dy = \gamma_{SL} \int_C \vec{e}.\vec{dl} \quad (5)$$

The vector integrand is $\vec{e} = \gamma_{SL} \cdot \begin{bmatrix} 0 \\ x.\frac{y}{R} \\ x.\frac{z}{R} \end{bmatrix}$

Drop volume During computation, the liquid drop is constrained to a fixed volume V . Since Evolver only models surfaces, V has to be calculated from the drop facets. This is done using the divergence theorem:

$$\iiint_V \text{div} \vec{F} \cdot dV = \oiint_S \vec{F} \cdot d\vec{S} \quad (6)$$

Since the drop volume is $\iiint_V dV$, we need to integrate on the surface a vector \vec{F} which satisfy $\text{div} \vec{F} = 1$. The solutions $\vec{F} = y \cdot \vec{e}_y$ or $\vec{F} = z \cdot \vec{e}_z$ are not correct because it will take into account volume of the wetted fiber (this is because the drop - fiber interface is not represented). Thus we need to use $\vec{F} = x \cdot \vec{e}_x$ and the volume is obtained through the following vector integral over the drop surface:

$$V = \oiint_S x \cdot \vec{e}_x \cdot d\vec{S} \quad (7)$$

Gravitational energy Since gravitational energy E_G is related to the drop volume, it is also computed using the divergence theorem (equation 6). We now have to solve $\vec{\nabla} \cdot \vec{F} = \rho \cdot g \cdot z$. Once again the general form $\vec{F} = \frac{1}{2} \rho \cdot g \cdot z^2 \cdot \vec{e}_z$ or the projection on y axis with $\vec{F} = \rho \cdot g \cdot y \cdot z \cdot \vec{e}_y$ cannot be used because it will partially take into account the fiber volume. As a consequence we use $\vec{F} = \rho \cdot g \cdot x \cdot z \cdot \vec{e}_x$ and gravitational energy is obtained from the following vector integral over the drop surface :

$$V = \oiint_S \rho \cdot g \cdot x \cdot z \cdot \vec{e}_x \cdot d\vec{S} \quad (8)$$

5.3 Model

```
// hanging_clamshell.fe  
// By R. Dufour, January 2012
```

```
VIEW_TRANSFORM_GENERATORS 2
```

```
-1 0 0 0      //x_mirror  
0 1 0 0  
0 0 1 0  
0 0 0 1
```

```
1 0 0 0      //y_mirror  
0 -1 0 0  
0 0 1 0  
0 0 0 1
```

```
// PARAMETERS – MKS system unit
```

```
parameter rodr = 1.170E-004 // fiber radius  
parameter angle = 8.000E+001 // contact angle with fiber  
parameter TENS = 7.280E-002 // Liquid surface tension  
parameter vol = 5.000E-010 // drop volume (cubic microliters)  
parameter dens = 998 // density of liquid
```

```
#define rode (-TENS*cos(angle*pi/180)) // liquid-rod contact energy  
#define ht vol^(1/3) // initial drop dimension  
#define wd vol^(1/3) // initial drop dimension
```

```
gravity_constant 9.81 // gravity is 9.81 m/s^2  
gap_constant 0.001 // to avoid wrapping around fiber  
scale_limit 0.5 // scale factor.
```

```
// VOLUME AND GRAVITATIONAL ENERGY
```

```
//volume
```

```
quantity fvint fixed = 0.25*vol method facet_vector_integral global  
vector_integrand:
```

```
q1: x  
q2: 0  
q3: 0
```

```
// Gravitational energy
```

```
quantity grav_x energy modulus dens method facet_vector_integral global
vector_integrand:
q1: G*x*z
q2: 0
q3: 0

// CONSTRAINTS -----

constraint 1 convex // Fiber surface
formula: y^2 + z^2 = rodr^2
energy:
e1: 0
e2: -rode*x*z/rodr
e3: rode*x*y/rodr

constraint 2 // Vertical symmetry plane (x_mirror)
formula: x = 0

constraint 3 nonnegative // Fiber surface (to prevent caving in)
formula: y^2 + z^2 = rodr^2

constraint 4 // Vertical symmetry plane (y_mirror)
formula: y = 0

// INITIAL GEOMETRY -----

vertices
1 0 -wd 0 constraint 2 // equatorial vertices
2 0 0 -wd constraint 2,4
3 ht -wd 0 // upper outer corners
4 ht 0 -wd constraint 4
5 0 -rodr 0 constraint 1,2 // lower vertices on rod
6 ht -rodr 0 constraint 1 // upper vertices on rod
7 ht 0 -rodr constraint 1,4

edges
1 1 2 constraint 2 // equatorial edges
4 5 1 constraint 2
5 3 4 // upper edges
9 6 7 constraint 1
10 6 3 // upper edge
11 1 3 // vertical external edges
12 2 4 constraint 4
```

```
14 5          6          constraint 1 // vertical internal edges
16 4          7          constraint 4 // cutting top plane

faces
1 1 12 -5 -11      tension TENS      constraint 3 // side faces
4 4 11 -10 -14     tension TENS      constraint 3
6 5 16 -9 10       tension TENS      constraint 3

bodies
1 1 4 6
```

5.4 Critical volume computation

To obtain the maximal volumes of hanging drop, the above model was run from a C++ program and dichotomy method was used to get Ω_c with a accuracy of $0.1 \mu L$. For each volume, an evolving procedure was used (not shown here), consisting in a sequence of evolution and refinement steps. Progressive refinement along z axis was used because of important difference deformation length-scale (typically $\approx 10 \mu m$ mesh element size was used around the fiber and $\approx 100 \mu m$ was used for the bottom part of the drop).

We assumed equilibrium was achieved when reaching a 10^{-10} % variation in energy, in that case the probe volume was increased. Otherwise divergence was observed by mean of drop detachment from the fiber.

It is to be noted that, from a general point of view, the drop fiber system can exhibit two different stable configurations, corresponding to the barrel or clamshell drop shape. For the range of contact angle investigated in this paper (θ ranging from 80° to 120°), the system can only present a barrel configuration (Energy phase diagram and stability were previously studied by Chou et al.⁴, also achievement of a clamshell drop is possible only for small contact angles, typically $\theta < 50^\circ$).

Thereby we expect only two cases: the droplet reaches the barrel configuration, which corresponds to a local minimum of energy, or it falls from the fibers, and in that case the total energy keeps decreasing and never reaches a minimum. These two cases are represented from an energetically point of view in figure 9. System energy is represented as a function of the drop fiber contact length. Depending on the starting point of the simulation, the numerical method can converge either to the barrel configuration or to the falling off of the droplet. Because the numerical method uses energy gradient descent, starting points B and C in the example of figure 9 will converge to the barrel drop while starting point A will result in drop fall, without finding the metastable barrel state.

To avoid this problem of bi-stability, it is preferable to get the initial drop configuration close to point C, so that if a metastable barrel shape exists, it will not be missed during energy minimization. For this reason the initial drop shape used for the simulations presents an important drop fiber contact length (shown below), which corresponds to point C in figure 9. Thereby during shape evolution it will converge to the barrel configuration if the latter exists, otherwise the contact length decreases down to 0, leading to a spherical droplet disconnected from the fiber (shown below).

References

- 1 R. Dufour, M. Harnois, Y. Coffinier, V. Thomy, R. Boukherroub and V. Senez, *Langmuir*, 2010, **26**, 17242–17247.
- 2 R. Dufour, M. Harnois, V. Thomy, R. Boukherroub and V. Senez, *Soft Matter*, 2011, **7**, 9380–9387.
- 3 E. Lorenceau, C. Clanet and D. Quere, *J. Colloid Interf. Sci.*, 2004, **279**, 192–197.
- 4 T. H. Chou, S. J. Hong, Y. E. Liang, H. K. Tsao and Y. J. Sheng, *Langmuir*, 2011, **27**, 3685–3692.

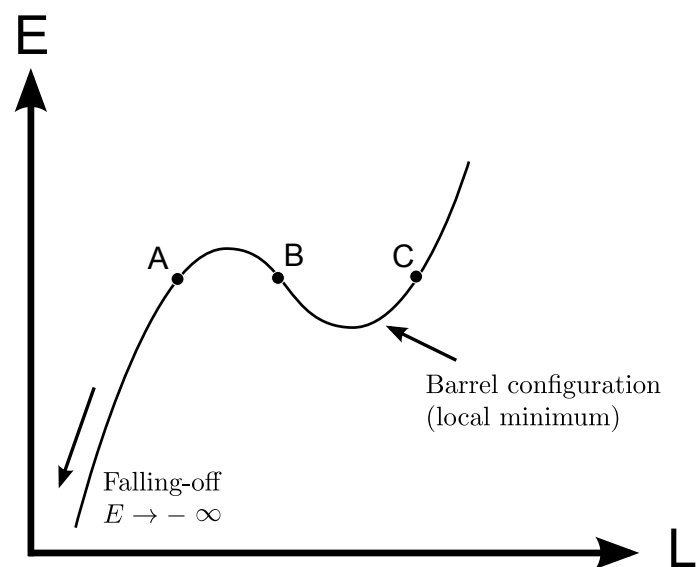


Fig. 9 Energy landscape for the drop on fiber system. Depending on the starting point A, B or C, the numerical method (energy gradient descent) can result in the barrel configuration or falling off of the droplet.

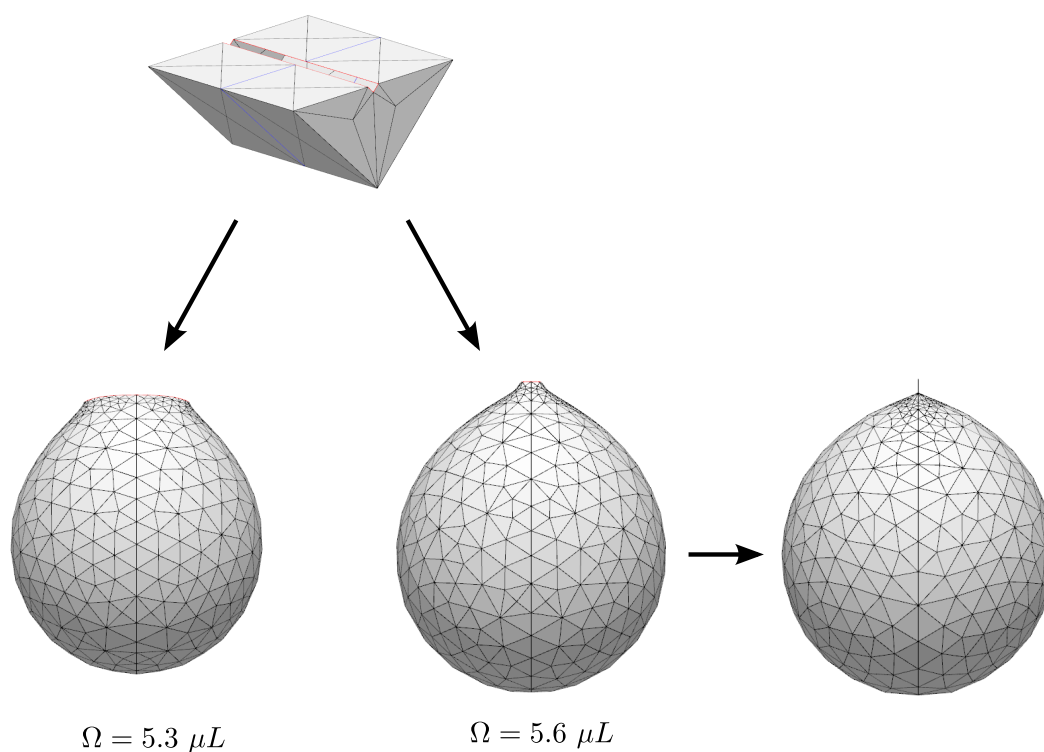


Fig. 10 Top: initial drop shape before evolution. The initial drop fiber contact length is important so that the numerical method cannot miss the metastable barrel configuration. In this example the contact angle is $\theta = 100^\circ$. For a volume $\Omega = 5.3 \mu L$, the numerical method converges to the barrel shape (bottom left) while for a slightly larger volume $\Omega = 5.6 \mu L$, contact length decreases down to 0 and drop falls down (remaining attached to the fiber by a single edge).